www.czasopisma.pan.pl PAN POLSKA AKADEMIA NAUK www.journals.pan.pl

Arch. Metall. Mater., Vol. 61 (2016), No 3, p. 1437–1440

DOI: 10.1515/amm-2016-0235

K. KOWALSKI*#, M. NOWAK*, M. JURCZYK*

MECHANICAL AND CORROSION PROPERTIES OF MAGNESIUM-BIOCERAMIC NANOCOMPOSITES

Magnesium alloys have recently attracted much attention as a new generation of biodegradable metallic materials. In this work, Mg1Mn1Zn0.3Zr-bioceramic nanocomposites and their scaffolds were synthesized using a combination of mechanical alloying and a space-holder sintering process. The phase and microstructure analysis was carried out using X-ray diffraction, scanning electron microscopy and the properties were measured using hardness and corrosion testing equipment. Nanostructured Mg-bioceramic composites with a grain sizes below 73 nm were synthesized. The Vickers hardnesses for the bulk nanostructured Mg-based composites are two times greater than that of pure microcrystalline Mg metal (50 HV0.3). Produced Mg-based bionanomaterials can be applied in medicine.

Keywords: Bionanocomposites, Magnesium, Bioceramics, Microstructure

1. Introduction

The number of medical implant placed has risen dramatically the past years due to a growing aging population and simplicity of treatment. Magnesium and its alloys have attracted a lot of attention as potential bone implant materials [1, 2]. However high reactivity and poor corrosion resistance in chloride containing solutions, including human body fluid, are the disadvantages [3].

One of the methods that allow the biological properties of Mg alloys to be altered is the modification of its chemical composition and microstructure. Magnesium is usually alloyed with other metals. Mn and Zn were selected as the alloying elements to develop Mg-Mn-Zn alloys due to its good biocompatibility. The addition of these metals improves not only the mechanical properties but also the corrosion resistance of magnesium alloys. On the other hand, Zr can readily decrease the grain size by 80% or even more under normal cooling rates [4]. The solubility of Zr in Mg is about 0.5 wt.%.

The other option is to produce a composite that will exhibit the favorable mechanical properties of Mg and the excellent biocompatibility and bioactivity of a ceramic [5]. The most commonly used ceramics employed in medicine are hydroxyapatite (HA; $Ca_{10}(PO_4)_6(OH)_2$) and bioglass (45S5 Bioglass (BG); 45% SiO_2, 24.5% Na_2O, 24.5 CaO, 6% P_2O_5). Recent studies have clearly demonstrated that the nanostructuring of metallic biomaterials can considerably improve not only its mechanical properties but also the biocompatibility [6]. The nanocrystalline structures can be produced by non-equilibrium processing technique such as mechanical alloying (MA) [7] or rapid solidification [8].

The mechanical alloying method and the powder metallurgy process for the fabrication of bulk Ni-free austenitic stainless steel-HA and Ti-HA nanocomposites with a unique microstructure have been developed [7, 9]. Independently, metal matrix composite (MMC) composed of magnesium alloy AZ91D as a matrix and hydroxyapatite particles as reinforcements have been examined [10].

Coatings of hydroxyapatite are often applied to metallic implants (titanium, titanium alloys and stainless steels) to alter the surface properties, but in many cases satisfactory results were not achieved, due to crack formation or badly controlled adjustment of the specific apatite phases. Latest studies have focused their attention on the possibility of its application in composite form, in materials uniting metal with ceramic [9−11]. Recently, the effect nano-hydroxyapatite contents (0-10 wt.%) on the microstructure and mechanical properties of magnesium nanocomposites densified by high frequency induction heat sintering was investigated [12]. Addition of 1 to 3 wt. % of HA improved compression strength of Mg by 16 %. Due to the agglomeration of HA particles, the compressive strength decreased, when the HA content was larger than 2 wt. %.

The present study examines the mechanical and corrosion properties of nanostructured Mg1Mn1Zn0.3Zr alloy through bioceramic (HA, or BG) alloying.

2. Materials and methods

The Mg1Zn1Mn0.3Zr-x wt.% bioceramic nanocomposites were prepared by mechanical alloying and powder metallurgy (bioceramic = HA or BG; x = 0, 5). Elemental powders of magnesium (99.8% purity, maximum particle size 45 μm; Alfa-Aesar), zinc (99% purity, maximum particle size 600 μm; Alfa-Aesar), manganese (99% purity, maximum particle size 45 μm; Alfa-Aesar), zirconium (95.0% purity, maximum particle size 350 μm; Ciech-Poland), hydroxyapatite (reagent grade; Sigma-Aldrich) and 45S5 Bioglass (53 μm, Mo-Sci Health Care L.L.C. USA) powder were used as starting materials.

* POZNAN UNIVERSITY OF TECHNOLOGY, INSTITUTE OF MATERIALS SCIENCE AND ENGINEERING, POZNAN, POLAND

** Corresponding author: kamil.h.kowalski@doctorate.put.poznan.pl

Mechanical alloying was carried out using a SPEX mixer mill, model 8000, employing a BPR of 10:1 for 20 h. In order to prevent severe cold welding during high-energy milling, the ball milling was stopped every 15 minutes to dissipate a heat and to reduce an excessive rise in temperature. These breaks in MA process were done also to crush bulk materials in vials as well as to scrape powder adhered to balls and walls. All these operations were carried out in the glove box filled with argon.

Bulk nanostructured Mg-based composites and its scaffolds were prepared using a powder metallurgy. In the first case, the powders were uniaxially pressed at compacting pressure of 600 MPa. The typical dimensions of the pellets were d = 8 mm in diameter and h = 3 mm in height. Finally, the green compacts were heat treated at 550 °C for 2 h under an argon atmosphere (99.999% purity) to form bulk samples. In the second case, the blended Mg-based powders were mixed with ammonium hydrogen carbonate (NH_4HCO_3), which was used as the space-holder material. The size of the space-holder particles was 500-800 μm. The mixture containing MA powder and NH_4HCO_3 was uniaxially pressed at a compacting pressure of 400 MPa. The resulting pellets were typically 8 mm in diameter and 5 mm in height. The green compacts were sintered under a vacuum of 10^{-4} Torr in two steps (at 175 °C for 2 h to remove the space-holder particles and finally the compacts were heat treated at 550 ºC for 2 h). Porous Mg-based composites with porosity of 40% were fabricated by adding 25 wt.% ammonium hydrogen carbonate to the powder mixtures.

Structure, microstructure, composition and morphology of materials were studied by X-ray diffraction (XRD), scanning electron microscopy (SEM) and transmission electron microscopy (TEM). XRD data of studied alloy, composites and scaffolds were obtained from Panalytical Empyrean with Cu Kα (λ = 1.54056 Å). XRD data were used to calculate average crystallite size by using Scherrer equation. SEM microscope was used to characterize the morphology of the prepared samples in function of milling time. The TEM images were recorded using a Philips CM 20 Super Twin microscope, which provides a 0.24 nm resolution at an acceleration voltage of 200 kV.

The Vickers microhardness of the bulk samples was measured using a microhardness tester by applying a load of 300 g on the polished surfaces of the samples. The nanomechanical property, Young's modulus of bulk Mg-based nanocomposites, was evaluated using a CSM Instruments nanoindenter with a Berkovich diamond tip. Using nanoindenter, the "indentation modulus" EIT parameter was estimated [13]. For evaluation of Young's modulus of porous Mg-based nanocomposites, tensile tests were performed at room temperature using a universal materials testing machine operating under a strain rate of 10-3s-1. The tensile test specimen was in accordance with the subsize ASTM E-8 standard.

The corrosion resistance in Ringer's solution was measured using *in vitro* potentiodynamic corrosion test. The composition of Ringer's solution was NaCl: 9g/l, KCl: 0.42 g/l, $CaCl_2$: 0.48 g/l, $NaHCO_3$: 0.2 g/l. The corrosion test was performed at 37±1 °C. The Solartron 1285 potentiostat was applied. The corrosion test was run in EG&G K0047 corrosion cell. The counter electrode consisted of two graphite rods and a saturated calomel electrode (SCE) was used as the reference electrode. The corrosion potentials (E_C) and corrosion current densities (I_C) were estimated from the Tafel extrapolations of the corrosion curves, using CorrView software.

3. Results and discussion

Mg1Zn1Mn0.3Zr-x wt.% bioceramic nanocomposites were prepared by MA and annealing process (x=0, 5). The behavior of MA process was studied by X-ray diffraction and microstructural investigations. Fig. 1 shows a series of XRD spectra of mechanically alloyed Mg1Zn1Mn0.3Zr-5 wt.% HA and Mg1Zn1Mn0.3Zr-5 wt.% BG nanocomposites powder mixture subjected to milling for increasing time (0 h – 20 h). The originally sharp diffraction lines of Mg gradually become broader and their intensity decreases with milling time. In Mg1Zn1Mn0.3Zr-5 wt.% HA composition the HA peaks almost disappeared for the sample milled for 1 h. After 20 h of MA, the Mg1Zn1Mn0.3Zr-5 wt.% HA sample is formed by a Mg solid solution with a c/a ratio 1.626. The peak positions for magnesium, the major phase, are shifted to higher angles, due to dissolution of Zn, Mn and Zr in the Mg matrix.

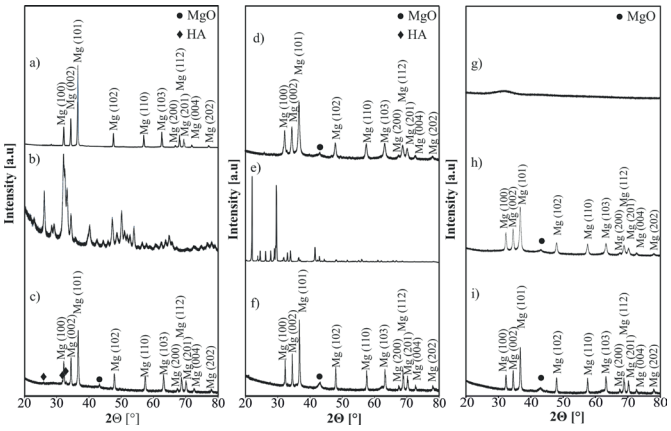

Fig. 1. XRD pattern of: pure Mg (a), hydroxyapatite powder (b), Mg1Zn1Mn0.3Zr-5 wt.% HA powder after 15 min of MA (c), Mg1Zn1Mn0.3Zr-5 wt.% HA nanocomposite after 20 h of MA (d), NH_4HCO_3 particles (e), Mg1Zn1Mn0.3Zr-5 wt.% HA porous scaffold with 40 % porosity (f), BG powder (g), Mg1Zn1Mn0.3Zr-5 wt.% BG after 20 h of MA (h) and Mg1Zn1Mn0.3Zr-5 wt.% BG bulk sample (i)

Fig. 2 (a-c) shows SEM pictures of obtained powdered Mg1Zn1Mn0.3Zr-5 wt.% HA materials, as an example. Lamellar structure was increasingly refined during MA process. Thickness of material layers decreases with increasing of MA time. After heat treatment, samples showed cleavage fracture morphology. Size distribution of Mg1Zn1Mn0.3Zr-5 HA particles varies from 20 to 200 micrometers. Size of Mg1Zn1Mn0.3Zr particles doesn't exceed 100 μm.

During the MA process the crystalline size of the magnesium decreases with MA time and reaches a steady value of about 45 nm after 20 h of milling (Table 1). Formation of the bulk and porous nanocrystalline composites were achieved by annealing the MA materials in high purity argon atmosphere at 550 °C for 2 h (Fig. 1, Fig. 2 d, e). For

Mg1Zn1Mn0.3Zr-5 wt.% HA and Mg1Zn1Mn0.3Zr-5 wt.% BG except main hexagonal type structure (hcc type) with cell parameters a = 3. 202 Å, c = 5. 299 Å and a = 3. 194 Å and c = 5. 186 Å MgO phase was detected, respectively. When HA or BG is added to Mg1Zn1Mn0.3Zr the lattice constant a and c decreases.

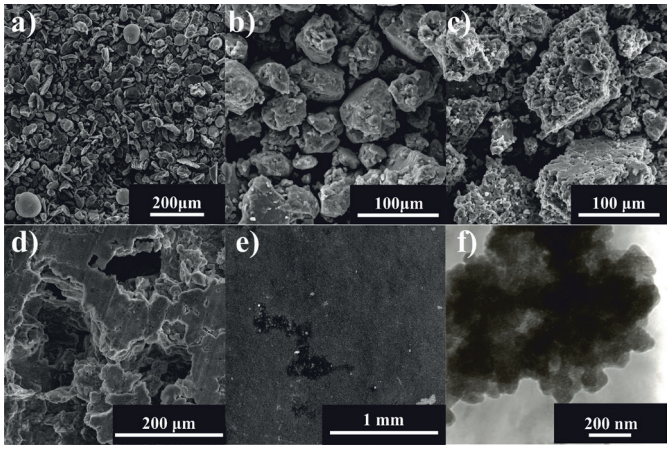

Fig. 2. SEM images of Mg1Zn1Mn0.3Zr-5 wt.% HA nanocomposite powders after: a) 0 min, b) 1h, c) 20h of MA process, d) porous scaffold with 40% porosity, e) bulk Mg1Zn1Mn0.3Zr-5 wt.% BG, f) TEM image of powder of Mg1Zn1Mn0.3Zr-5 wt.% HA milled for 20 h

Fig. 2. f) shows the TEM micrograph of the mechanically alloyed for 20 h and annealed at 550 ºC for 2 h Mg1Zn1Mn0.3Zr-5 wt.% HA powdered sample. Nanoparticles with the size below 100 nm on average are shown. As was measured by Scherrer formula, the crystal size of the bulk samples containing 5 wt.% HA and 5 wt.% BG were 45 and 60 nm, respectively.

The Vickers microhardness of the sintered Mg1Zn1Mn0.3Zr-5 wt.% bioceramic nanocomposites exhibited various distributions that were related to compositional changes, and the microhardness increased with an increase in the content of bioceramic. The Vickers hardnesses for the bulk nanostructured Mg1Zn1Mn0.3Zr-5 wt.% HA and Mg1Zn1Mn0.3Zr-5 wt.% BG nanocomposites reached 100 $HV_{0.3}$ and 81 $HV_{0.3}$, respectively, and are almost 2 times greater than that of pure microcrystalline Mg metal (50 $HV_{0.3}$). This effect is directly associated with structure refinement and obtaining a nanostructure.

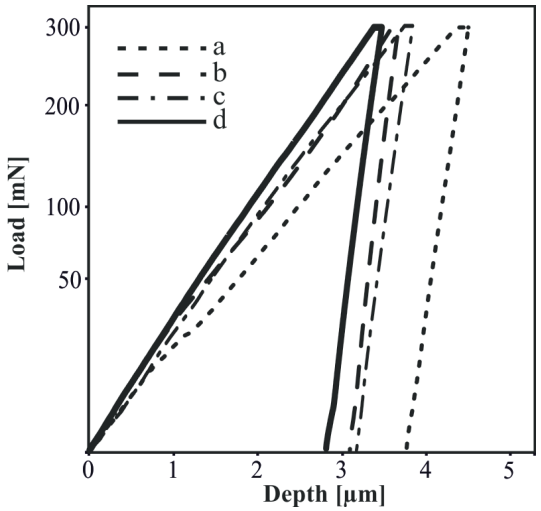

Fig. 3. Load-depth (F-d) nanoindentation curves of studied materials: bulk Mg (a), bulk Mg1Zn1Mn0.3Zr alloy (b), Mg1Zn1Mn0.3Zr-5 wt.% BG (c) and Mg1Zn1Mn0.3Zr-5 wt.% HA (d) obtained for applied load 300 mN

Nanomechanical property (Young's modulus) of Mg1Zn1Mn0.3Zr-5 wt.% bioceramic were performed on the non-etched specimens. The load vs. penetration depth curves are shown for the selected measurements (Fig. 3) for the bulk magnesium (Fig. 3a), nanocrystalline Mg1Zn1Mn0.3Zr alloy (Fig. 3b) and bulk Mg1Zn1Mn0.3Zr-5 wt.% HA and Mg1Zn1Mn0.3Zr-5 wt.% BG nanocomposites (Fig. 3c), respectively. All the indentation curves indicated the elastic–plastic behavior of the investigated materials. The higher average values of Young's modulus (49.13 GPa) characterize the Mg1Zn1Mn0.3Zr-5 wt.% HA nanocomposite. In case of the Mg1Zn1Mn0.3Zr-5 wt.% HA scaffold with 40% porosity, the Young's modulus is equal 30 GPa (Table 1).

The corrosion properties were potentiodynamically investigated in Ringer's solution at 37 °C and examples of polarization curves are shown on Fig. 4. Nanostructured Mg1Zn1Mn0.3Zr-5 wt.% BG composite was more corrosion resistant (I_C = 1.49·10^{-4} Acm^{-2}, E_c = -1.822V vs. SCE) than Mg1Zn1Mn0.3Zr-5 wt.% HA nanocomposite (I_C = 3.39·10^{-4} Acm^{-2}, E_c = -1.541V vs. SCE) (Table 1).

Several reports have shown that decreasing the corrosion rate of Mg in simulated body fluids is possible

TABLE 1

Properties of Mg- bioceramic nanocomposites

sample	d	HV0.3	E [GPa]	I_c [A/cm^2]	E_c [V]
Mg-Mn-Zn-Zr	73 nm	90	47.77	1.62·10-4	-1.777
Mg-Mn-Zn-Zr-5HA	45 nm	100	49.13	3.39·10-4	-1.541
Mg-Mn-Zn-Zr-5BG	60 nm	81	46.84	1.49·10-4	-1.822
Mg-Mn-Zn-Zr-5HA after HF immersion	-	-	-	2.43·10-4	-1.442
microcrystalline Mg	40 µm	50	38.38	3.34·10-4	-1.754

by surface treatment methods. Among different methods hydrofluoric acid treatment is a promising method owing to its simplicity and low cost [14]. By the application of HF treatment method, corrosion rate decreases by providing a magnesium fluoride (MgF_2) protective layer on the surface of the sample. Additionally, when Mg1Zn1Mn0.3Zr-5 wt.% HA nanocomposite is immersed in 40 % HF for 2h, formation of a protective MgF_2 layer over the surface occurs. On the other hand, the increased corrosion resistance was attributed to the formation of a natural magnesium oxide film (Table 1.).

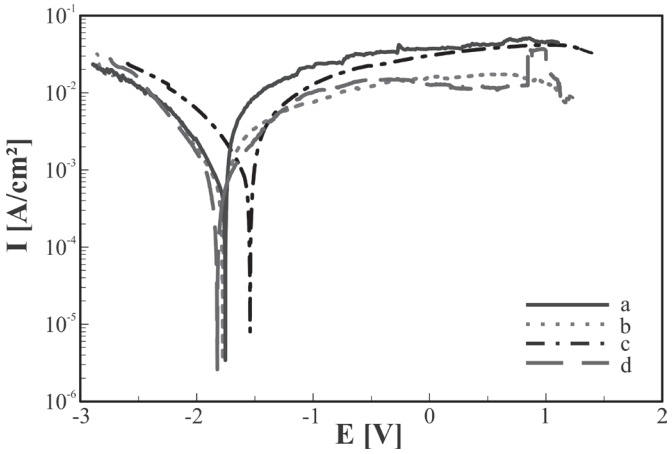

Fig. 4. Potentiodynamic curves of: pure Mg (a), Mg1Zn1Mn0.3Zr alloy (b), Mg1Zn1Mn0.3Zr-5 wt.% 5HA (c) and Mg1Zn1Mn0.3Zr-5 wt.% BG (d) nanocomposites

Mechanical alloying technique allows alloying of elements that are difficult or impossible to combine by conventional melting methods. These biomaterials possess unique mechanical and surface properties similar to the bone and hence are considered to be the future generation biomaterials.

4. Conclusion

A new kind of biomedical bulk and porous Mg1Mn1Zn0.3Zr-type nanocomposites with bioceramics were prepared by mechanical alloying and powder metallurgy process. An enhancement of the properties due to the nanoscale structure in a consolidated samples was observed. Mg-based scaffolds are more corrosion resistant than the bulk microcrystalline Mg in Ringer solution. The bulk and porous Mg1Zn1Mn0.3Zr- 5 wt. % bioceramic (BG or HA) nanocomposite, due to mechanical and corrosion properties would offer new structural and functional properties for innovative products in medical applications.

Acknowledgements

The work was financed by National Science Centre Poland under the decision no. DEC-2013/11/B/ST8/04394.

REFERENCES

[1] F. Witte. Acta Biomater. **6**, 1680–92 (2010).
[2] M. Li, Y.F. Zheng. J. Mater. Sci. Technol. **29**, 489–502 (2013).
[3] N. Li, C. Guo, Y.H. Wu, Y.F. Zheng, L.Q. Ruan. Corr. Eng. Sci. Techn. **47**, 346–351 (2012).
[4] Q. Ma, D. Graham, L. Zheng, D.H. StJohn, M.T. Frost Mater. Sci. Tech.-Lond. **19**, 156–162 (2003).
[5] W.P. Cao, L. Hench, Ceram. Int. **22**, 493-507 (1996).
[6] B.C. Ward, T.J. Webster. Mat. Sci. Eng. C **27**, 575–578 (2007).
[7] M. Tulinski, M. Jurczyk. Appl. Surface Sci. **260**, 80– 83 (2012).
[8] M. Szymanek, B. Augustyn, D. Kapinos, S. Boczkal, J. Nowak. Arch. Metal. Mater. **59**, 317–321 (2014).
[9] K. Jurczyk, G. Adamek, M.M. Kubicka, J. Jakubowicz, M. Jurczyk. Materials **8**, 1398–1412 (2015).
[10] F. Witte, F. Feyerabed, P. Maier, J. Fischeer, M. Stömer, C. Blawert, W. Dietzel, N. Hort. Biomaterials **28**, 2163–2174 (2007).
[11] K.A. Khalil, Int. J. Electrochem. Sci. **7**, 10698–10710 (2012).
[12] A.K. Khanra, K.C. Jung, S.H. Yu, K.S. Hong, K.S. Shin. Bull. Mater. Sci. **33**, 43–47 (2010).
[13] A.C. Fisher-Cripps. Nanoindentation. 3rd ed., Springer, New York (2011).
[14] M. Razavi, M.H. Fathi, M. Meratian. Mater. Charact. **61**, 1363–1370 (2010).